Alma Mater Studiorum · Università di Bologna

Scuola di Scienze
Dipartimento di Fisica e Astronomia
Corso di Laurea in Fisica

Tidal response and Love numbers of the Moons of Uranus

Relatore:
Prof. Giorgio Spada

Presentata da:
Luca Francioni

Anno Accademico 2023/2024

Abstract

Le maree solide sono veri e propri sollevamenti e abbassamenti della superficie di un corpo planetario, causati dall'azione delle forze gravitazionali esercitate da corpi esterni. Tali deformazioni, in aggiunta alla variazione di potenziale che ne consegue, sono parametrizzate da tre coefficienti adimensionali chiamati numeri di Love, che descrivono la suscettibilità del corpo planetario alla deformazione mareale e dipendono direttamente dalle caratteristiche fisiche di quest'ultimo. In questa tesi è presentato lo studio delle maree solide delle lune di Urano, corpi planetari di estremo interesse per diverse missioni spaziali programmate per il prossimo futuro. Tali corpi sono descritti attraverso un modello planetario elastico, omogeneo, incomprimibile, e di forma sferica. Dopo aver presentato le proprietà fisiche di ogni luna, attraverso un'analisi grafica e numerica stimiamo i loro numeri di Love e i relativi spostamenti della superficie all'equatore e ai poli delle stesse. Per le lune più piccole e vicine a Urano otteniamo numeri di Love relativamente piccoli ma spostamenti della superficie notevoli mentre per le lune più grandi troviamo valori maggiori per i numeri di Love, simili a quelli di modelli differenziati della nostra Luna, e valori minori per gli spostamenti della superficie; le lune più distanti, nonostante abbiano numeri di Love dello stesso ordine di grandezza delle lune vicine, sono così distanti dal pianeta da presentare valori di spostamento superficiale trascurabili. Vengono infine proposti alcuni miglioramenti al modello planetario presentato in questa tesi che, alla conoscenza del relatore e dell'autore, è il primo lavoro ad avere come obiettivo la stima comparativa e sistematica dei numeri di Love e delle ampiezze di deformazione superficiale di tutte le lune di Urano.

Abstract

Body tides are lifting and lowering phenomena of the solid surface of a planetary body, caused by the action of the gravitational forces exerted by external bodies. Such deformations, in addition to the perturbation of the gravitational potential of the body that follows, are parameterized by three dimensionless coefficients called Love numbers, that describe the susceptibility of the planetary body to tidal deformations and depend directly on the physical properties of this latter. In this dissertation we present the study of the body tides of the moons of Uranus, planetary bodies that are extremely interesting for many space missions scheduled for the near future. We describe these satellites using an elastic, homogeneous and incompressible planetary model, in spherical shape approximation. After presenting the physical properties of each moon, through a graphical and numerical analysis we evaluate their Love numbers and the relative surface displacements at their equator and poles. For the smallest moons that are near to Uranus, we obtain relatively small Love numbers and great surface displacements while for the major moons we obtain greater values of Love numbers, similar to the ones of differentiated models of our Moon, and smaller values of surface displacements; for the outer moons, despite they have Love numbers values of the same order of magnitude of the inner smallest ones, they are so far from Uranus that their values of surface displacements are negligible. In the end, we propose some improvement scenarios for the model we have presented in this dissertation, that, to the knowledge of the supervisor and the author, is the first work having the comparative aim of systematically evaluating Love numbers and surface displacements of all the moons of Uranus.

Contents

1 Introduction

The knowledge of our Solar System, crucial to understand the dynamics of formation and evolution of our planet and beyond, is not as advanced as one might think today, especially regarding its outer regions. The only space mission capable of obtaining observational data about the planetary systems of Uranus and Neptune, the farthest planets from the Sun, was *NASA Voyager 2* in 1986: after exploring Jupiter and Saturn, its journey was extended to an orbit that facilitated its approach to the "ice giants", those extremely large planets, *i. e.* Uranus and Neptune, predominantly composed of water, ammonia and methane, generally called "ices" in Astrophysics (they are heavier species than hydrogen and helium - "gases" - but lighter than silicon and iron - "rocks" and "metals").

Thanks to the advancement in observation capabilities of extra-solar planetary systems, it has been understood that ice giants are a widespread planetary type in the Universe. Therefore, the interest of scientific community in them has steadily increased, becoming one of the main investigation priorities of space agencies like NASA and ESA.
In this regard, *NASA Uranus Orbiter and Probe* space mission, scheduled for launch in the 2030s, has gained great importance in the current research landscape: its objective is to investigate as many parameters as possible concerning the internal structure and dynamics of Uranus and its natural satellites (composition and distribution of mass, atmosphere, etc.) through the deployment of an orbiter and many atmospheric probes on the planet. A study like this is not only important to obtain an in-depth analysis of the ice giant itself, but also to confirm the presence of liquid water on its moons, already theorized by various planetary models based on observational data.
The desired approach for the theoretical and experimental preparation of this mission is the transversality of investigation, as also highlighted in the *Uranus Flagship 2023* conference (see *https://www.hou.usra.edu/meetings/uranusflagship2023/*): synergy between astronomers, astrophysicists and geophysicists is considered fundamental to reach all the objectives of *Uranus Orbiter and Probe* mission, both for those of technical realization of the orbiters and for those of the mission itself.

The aim of the following dissertation is the evaluation of one of the most important properties of planetary dynamics: the deformative response of the moons of Uranus caused by the tidal forces exerted by the planet, through the evaluation of their tidal Love numbers. In *Section 2* I introduce the considered planetary bodies, with their classification and physical properties, and the model we have used. In *Section 3* I review the basic physical theory of solid tides. In *Section 4* I show the analytical methods that we have used to evaluate Love numbers, whose values are reported and discussed in *Section 5.* Finally, I summarize the conclusions in *Section 6*, also suggesting other possible approaches to improve the evaluation of Love numbers.

2 Natural satellites of Uranus

2.1 Classification

The satellite system of Uranus consists of 27 main moons, whose names come from William Shakespeare's plays: the largest moons were observed for the first time by W. Herschel in 1787, who discovered the planet itself six years before, and W. Lassell in 1851 while most of the smaller ones were discovered through the images of *NASA Voyager 2* space mission in 1986 [Smith et al., 1986] and observations in the ensuing decades. Astronomical observations of Uranus still reserve new discoveries of small celestial bodies orbiting the ice giant [CarnegieScience, 2024].
The main adopted classification of these moons is based on their distance from the planet and on their following orbital and physical properties:

- **<u>Inner moons</u>**
  Cordelia, **Ophelia**, **Bianca**, **Cressida**, **Desdemona**, **Juliet**, **Portia**, **Rosalind**, **Cupid**, **Belinda**, **Perdita**, **Puck**, **Mab** (in order of distance from Uranus).
  These orbiting bodies are relatively small and it is assumed that they were formed from the fragmentation of some pre-existing moon; their orbits are chaotic, self-perturbing and apparently instable, so in the next millions years possible collisions are not ruled out [Duncan and Lissauer, 1997]. Their surface composition is primarily composed by ice and other rocky materials [Dumas et al., 2003];

- **<u>Major moons</u>**
  Miranda, **Ariel**, **Umbriel**, **Titania**, **Oberon** (in order of distance from Uranus).
  They are the largest moons of the ice giant, probably formed with the planet itself or maybe detached from it after a collision event [Mousis, 2004]; their orbits are almost circular and almost coplanar to the equator of Uranus. They all seem to have no atmosphere, although some of them have active emission of CO_2 from the surface [Grundy et al., 2003, Cartwright et al., 2015]. On a geological and structural level, they are the most interesting satellites because they all show evident geophysical formations on the surface [Plescia, 1987, Croft, 1989, Schenk, 1991, Grundy et al., 2006] and some of them are possible candidates for hosting oceans of liquid water under their icy and rocky surfaces [Castillo-Rogez et al., 2023];

- **<u>Outer moons</u> (or irregular moons)**
  Francisco, **Caliban**, **Stephano**, **Trinculo**, **Sycorax**, **Margaret**, **Prospero**, **Setebos**, **Ferdinand** (in order of distance from Uranus).
  Due to their differences in mass and dimension, the main hypothesis about their nature is that these moons were not formed with the planet itself, but they were caught in orbit afterwards [Sheppard et al., 2005]. Their orbits are very large and irregular.

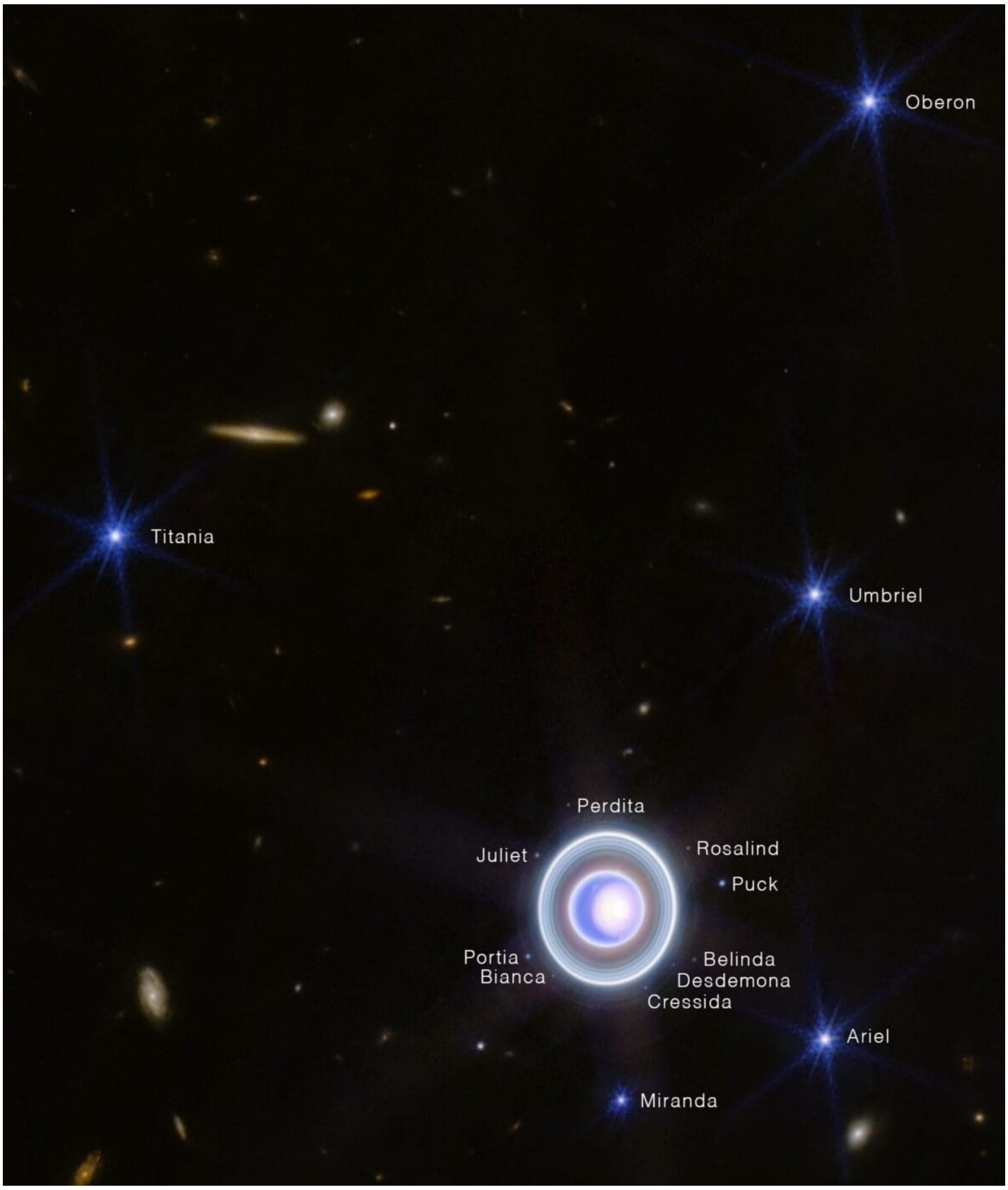

Figure 1: *The system of inner and major moons orbiting Uranus, captured by the James Webb Space Telescope. Sep. 4, 2023. NASA, ESA, CSA, STScI.*

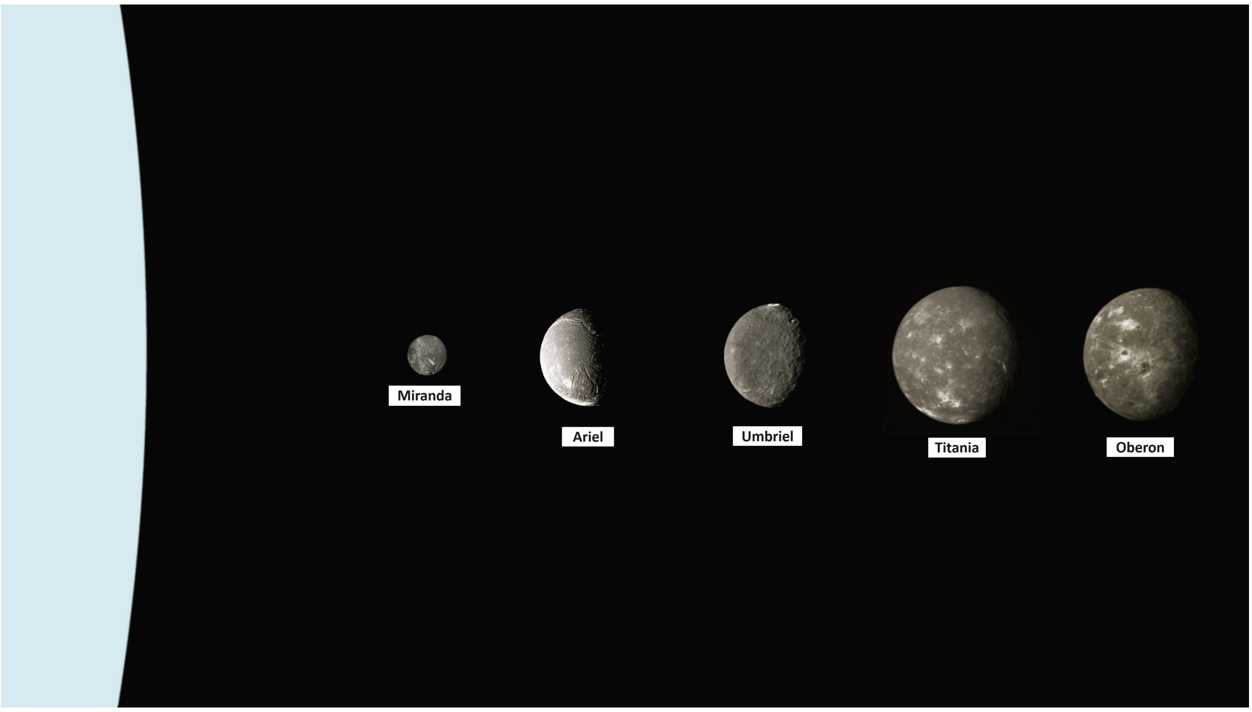

Figure 2: *Composed image of the major moons of Uranus, compared in size with the planet (visualized on the left); orbital distances are not in scale. Note that the radius of our Moon is about twice as large as the one of Oberon. The images of the moons are taken from the original figures captured by the NASA Voyager 2 mission. Jan. 24, 1986. NASA/JPL.*

2.2 Properties

In the following discussion, every moon is considered as:

- elastic;
- homogeneous, *i. e.* with uniform mass composition;
- incompressible, *i. e.* with constant density;
- in a spherical unperturbed state,

so that the following relation for the density ρ holds:

$$\rho = \frac{M}{\frac{4}{3}\pi R^3} , \tag{1}$$

where R is the radius and M is the mass of the moon.
The surface gravity g is:

$$g = \frac{GM}{R^2} , \tag{2}$$

where $G = 6.67 \cdot 10^{-11} \frac{N \cdot m^2}{kg^2}$ is the universal gravitational constant.

Physical data of the Uranian satellites are reported in Tables 1, 2 and 3, according to the classification of Section 2.1. The greatest density values are associated to those moons that present the most relevant rocky mass components, like the major ones. Density values assumed to be $1 \frac{g}{cm^3}$ are associated to moons that mainly present icy mass components; in fact, observational data showed that these ices are ammonia and carbon dioxide, as well as water ice [Grundy et al., 2006].

Rotational data of inner and outer moons are not available due to the lack of measurements and observations. For major moons, rotational data are reported in Table 4; in particular, each angular rotation speed ω was evaluated according to:

$$\omega = \frac{2\pi}{T} , \tag{3}$$

thanks to the fact that these moons are tidally locked, *i. e.* their orbital period of revolution T around Uranus is equal to that of rotation around their own axis [Smith et al., 1986].

Orbital data of all moons, *i. e.* their semi-major orbital axis a, are reported in Table 5.

Moon	$\boldsymbol{R}$ (km)	$\boldsymbol{M}$ $(10^{16}\,kg)$	$\boldsymbol{\rho}$ $(\frac{g}{cm^3})$	$\boldsymbol{\rho_{Fr}}$ $(\frac{g}{cm^3})$	$\boldsymbol{g}$ $(10^{-3}\,\frac{m}{s^2})$
Cordelia	21 ± 3	6.08 ± 0.57	1.57 ± 0.82	1.79	9.20 ± 3.49
Ophelia	23 ± 4	3.57 ± 0.32	0.70 ± 0.43	0.87	4.50 ± 1.97
Bianca	27 ± 2	6.38 ± 1.91	0.77 ± 0.40	0.90	5.84 ± 2.61
Cressida	41 ± 2	18.39 ± 2.12	0.64 ± 0.17	0.70	7.30 ± 1.55
Desdemona	35 ± 4	12.37 ± 4.63	0.69 ± 0.49	0.90	6.74 ± 4.06
Juliet	53 ± 4	38.71 ± 8.91	0.62 ± 0.28	0.90	9.19 ± 3.50
Portia	70 ± 4	116.71 ± 17.30	0.81 ± 0.26	0.90	15.89 ± 4.17
Rosalind	36 ± 6	17.59 ± 5.52	0.90 ± 0.73	0.90	9.05 ± 5.86
Cupid	~ 9	~ 0.31	1	-	2.55
Belinda	45 ± 8	24.71 ± 8.07	0.65 ± 0.56	0.90	8.14 ± 5.55
Perdita	15 ± 3	1.41	1	-	4.18
Puck	81 ± 2	191 ± 64	0.86 ± 0.35	0.90	19.42 ± 7.47
Mab	~ 12	~ 0.72	1	-	3.34

Table 1: **Physical data of inner moons**
Radius values R are reported from [Karkoschka, 2001] except for those of Cupid and Mab, taken from [Showalter and Lissauer, 2006]. Mass values M are reported from [French et al., 2024] except for those of Puck, taken from [Jacobson, 2023], and of Cupid, Perdita and Mab, indirectly computed from the density, assumed equal to $1\,\frac{g}{cm^3}$. Density values ρ are computed according to Eq. (1) and compared with values ρ_{Fr} taken from [French et al., 2024]. Surface gravity values g are computed according to Eq. (2). Uncertainties on ρ and g are evaluated by propagation of uncertainty as discussed in Appendix A.

Moon	$\boldsymbol{R}$ (km)	$\boldsymbol{M}$ ($10^{16}\,kg$)	$\boldsymbol{\rho}$ ($\frac{g}{cm^3}$)	$\boldsymbol{g}$ ($10^{-3}\,\frac{m}{s^2}$)
Miranda	235.8 ± 0.7	6293 ± 300	1.15 ± 0.06	75.49 ± 4.05
Ariel	578.9 ± 0.6	123310 ± 1800	1.52 ± 0.04	245.42 ± 4.09
Umbriel	584.7 ± 2.8	128850 ± 2250	1.54 ± 0.05	251.39 ± 6.80
Titania	788.9 ± 1.8	345500 ± 5090	1.68 ± 0.03	370.28 ± 7.14
Oberon	761.4 ± 2.6	311040 ± 7490	1.68 ± 0.06	357.86 ± 11.06

Table 2: **Physical data of major moons**
Radius values R are reported from [Thomas, 1988]. Mass values M are reported from [Jacobson, 2023]. Density values ρ are computed according to Eq. (1). Surface gravity values g are computed according to Eq. (2). Uncertainties on ρ and g are evaluated by propagation of uncertainty as discussed in Appendix A.

Moon	$\boldsymbol{R}$ (km)	$\boldsymbol{M}$ ($10^{16}\,kg$)	$\boldsymbol{\rho}$ ($\frac{g}{cm^3}$)	$\boldsymbol{g}$ ($10^{-3}\,\frac{m}{s^2}$)
Francisco	~ 11	~ 0.56	1	3.07
Caliban	~ 36	~ 19.54	1	10.06
Stephano	~ 16	~ 1.72	1	4.47
Trinculo	~ 9	~ 0.31	1	2.51
Sycorax	~ 75	~ 176.71	1	20.95
Margaret	~ 10	~ 0.42	1	2.79
Prospero	~ 25	~ 6.54	1	6.98
Setebos	~ 24	~ 5.79	1	6.71
Ferdinand	~ 10	~ 0.42	1	2.79

Table 3: **Physical data of outer moons**
Radius values R are reported from [Sheppard et al., 2005]. Mass values M are computed indirectly from the density ρ, assumed equal to $1\,\frac{g}{cm^3}$. Surface gravity values g are computed according to Eq. (2).

Moon	$\boldsymbol{T}$ $(days)$	$\boldsymbol{\omega}$ $(\frac{rad}{day})$	$\boldsymbol{\omega}$ $(10^{-5}\ \frac{rad}{s})$
Miranda	1.41	4.44	5.14
Ariel	2.52	2.49	2.89
Umbriel	4.14	1.52	1.75
Titania	8.71	0.72	0.84
Oberon	13.46	0.47	0.54

Table 4: **Rotational data of major moons**
Period values T are reported from [NASA, 2024]. Angular rotation speed values ω are computed according to Eq. (3), both in units of $\frac{rad}{day}$ and in units of $\frac{rad}{s}$.

Moon	$\boldsymbol{a}$ $(10^3\,km)$
Cordelia	49.8
Ophelia	53.8
Bianca	59.2
Cressida	61.8
Desdemona	62.7
Juliet	64.4
Portia	66.1
Rosalind	69.9
Cupid	74.4
Belinda	75.3
Perdita	76.4
Puck	86.0
Mab	97.7

Moon	$\boldsymbol{a}$ $(10^5\,km)$
Miranda	1.299
Ariel	1.909
Umbriel	2.660
Titania	4.363
Oberon	5.834
Francisco	42.757
Caliban	71.670
Stephano	79.514
Trinculo	85.026
Sycorax	121.932
Margaret	144.250
Prospero	162.210
Setebos	175.198
Ferdinand	204.214

Table 5: **Orbital data of the moons of Uranus**
Semi-major orbital axis values a are reported from [NASA, 2024], according to the classification presented in Sect. 2.1.

3 Theory of tides and Love numbers

To introduce the goals of this dissertation, the dimensionless parameters called Love numbers, it follows an introduction on Body tides Physics based on [Agnew, 2005] and [Spada, 2023]. Here, the discussion is contextualized to the case of the moons of Uranus.

3.1 Tidal forces

Consider a spherical, elastic, uniform and non-rotating celestial body of mass M, located at a certain distance from another mass M_p that acts as a "perturbing" mass on every surface point of the celestial body. In our case, think of M as the mass of a Uranian moon perturbed by the mass M_p of Uranus, as shown in Figure 3, where:

- O is a point mass m on the surface of the moon;
- C is the center of mass of the moon;
- U is the center of mass of the planet (considered as a point mass, due to the large orbital distance between each moon and Uranus);
- B is the center of mass of the moon-planet system.

In the reference system with origin B and rotating as the moon around the planet with angular velocity $\vec{\omega}$, we call *tidal force* $\vec{F}_t$ acting on O the sum of three forces:

1. the gravitational attraction force exerted by the planet $\vec{F}_{p,O}$;
2. the gravitational attraction force exerted by the moon $\vec{F}_{g,O}$;
3. the centrifugal force $\vec{F}_{cf}$, directed outwards $\overrightarrow{HO}$ where H is the projection of O on the axis of rotation.

It follows that:

$$\vec{F}_t = \vec{F}_{p,O} + \vec{F}_{g,O} + \vec{F}_{cf} = \vec{F}_{p,O} + \vec{F}_{g,O} + m\omega^2\overrightarrow{HO}\,. \tag{4}$$

Since $\overrightarrow{HO} = \overrightarrow{BO} - \overrightarrow{BH}$, with $|\overrightarrow{BH}| \ll |\overrightarrow{BO}|$ and $\overrightarrow{BO} = \overrightarrow{BC} + \overrightarrow{CO}$, and neglecting the radially directed terms with respect to C ($\vec{F}_{g,O}$ and $m\omega^2\overrightarrow{CO}$ cause a purely uniform radial uplift, so not a body tide), we have:

$$\vec{F}_t = \vec{F}_{p,O} + m\omega^2\overrightarrow{BC}\,. \tag{5}$$

Since C experiences no tidal force, we have:

$$\vec{F}_{t,C} = \vec{F}_{p,C} + m\omega^2\overrightarrow{BC} = 0 \implies m\omega^2\overrightarrow{BC} = -\vec{F}_{p,C}\,. \tag{6}$$

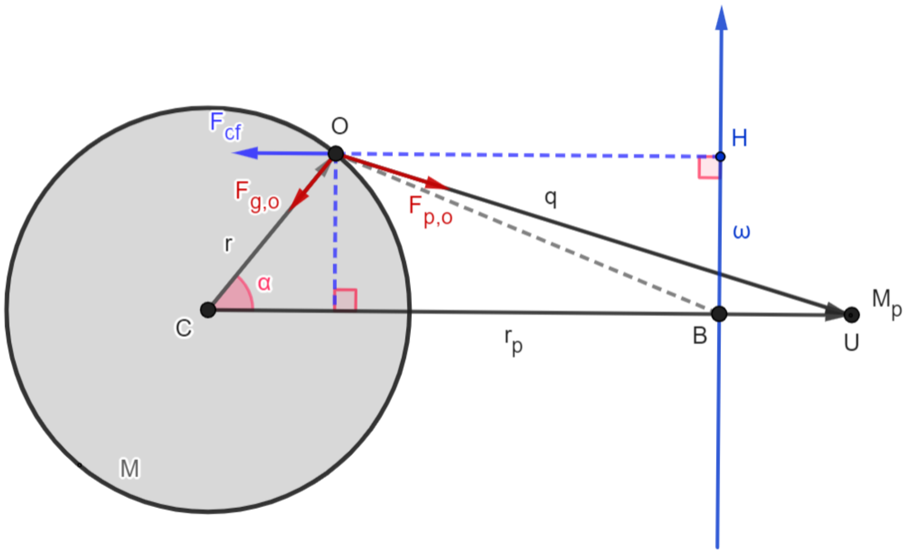

Figure 3: *Graphical representation of the forces acting on a point mass O on the surface of a moon, with Uranus assumed as the mass point U.*

Replacing (6) into Eq. (5), it is possible to express the tidal force as:

$$\vec{F}_t = \vec{F}_{p,O} - \vec{F}_{p,C}\,, \tag{7}$$

showing that the tidal force acting on a point O on the surface of the moon is due to the difference in gravitational attraction exerted by the planet on point O compared to that exerted on the center of mass C of the moon.

3.2 Tide rising potential

Renaming $\overrightarrow{CO} = \vec{r}$, $\overrightarrow{CU} = \vec{r}_p$ and $\overrightarrow{OU} = \vec{q}$, with magnitudes r, r_p and q respectively, and using the definition of gravitational force in Eq. (7), we have:

$$\vec{F}_t = \frac{GM_p m}{q^2}\frac{\vec{q}}{q} - \frac{GM_p m}{r_p^2}\frac{\vec{r}_p}{r_p} = GM_p m\left(\frac{\vec{q}}{q^3} - \frac{\vec{r}_p}{r_p^3}\right)\,, \tag{8}$$

so that, by Newton's second law, we can define the *tidal acceleration* in O as:

$$\vec{a}_t = \frac{\vec{F}_t}{m} = GM_p\left(\frac{\vec{q}}{q^3} - \frac{\vec{r}_p}{r_p^3}\right)\,. \tag{9}$$

In particular, the tidal acceleration can be expressed as the gradient of an appropriate potential, referred to as *tide rising potential*:

$$\Omega_t = GM_p\left(\frac{1}{q} - \frac{\vec{r}\cdot\vec{r}_p}{r_p^3} - \frac{1}{r_p}\right)\,. \tag{10}$$

Indeed, noting that $\vec{r}_p = \vec{q} + \vec{r} = const.$ and $\vec{q} = q\widehat{q}$, where $\widehat{q}$ is a unit vector, it follows that:

$$\begin{aligned}
\vec{\nabla}\Omega_t &= GM_p \left(\vec{\nabla} \left(\frac{1}{q} \right) - \vec{\nabla} \left(\frac{\vec{r} \cdot \vec{r}_p}{r_p^3} \right) - \vec{\nabla} \left(\frac{1}{r_p} \right) \right) = \\
&= GM_p \left(\vec{\nabla} \left(\frac{1}{q} \right) - \frac{\vec{r}_p}{r_p^3} \right) = \\
&= GM_p \left(\frac{\vec{q}}{q^3} - \frac{\vec{r}_p}{r_p^3} \right) = \\
&= \vec{a}_t \,. \qquad (11)
\end{aligned}$$

The tide rising potential can also be written as a series of Legendre polynomials in the variable $\cos\alpha$, where α is the angle between $\vec{r}$ and $\vec{r}_p$, *i. e.* the colatitude referred to U, as follows.
From Eq. (10), applying the cosine formula to OCU triangle we have:

$$q^2 = r_p^2 - 2r_p r \cos\alpha + r^2 = r_p^2 \left(1 - 2\frac{r}{r_p} \cos\alpha + \left(\frac{r}{r_p} \right)^2 \right) , \qquad (12)$$

hence:

$$\frac{1}{q} = \frac{1}{r_p} \left(1 - 2\frac{r}{r_p} \cos\alpha + \left(\frac{r}{r_p} \right)^2 \right)^{-\frac{1}{2}} . \qquad (13)$$

The term within parentheses is the generating function of the Legendre polynomials of $\cos\alpha$, valid for $\frac{r}{r_p} \leqslant 1$, in the form:

$$\frac{1}{q} = \frac{1}{r_p} \sum_{n=0}^{\infty} \left(\frac{r}{r_p} \right)^n P_n(\cos\alpha) \,. \qquad (14)$$

Expressing the dot product in Eq. (10) as:

$$\frac{\vec{r} \cdot \vec{r}_p}{r_p^3} = \frac{r r_p \cos\alpha}{r_p^3} = \frac{r}{r_p^2} \cos\alpha \,, \qquad (15)$$

we can write the tide rising potential as:

$$\Omega_t = \frac{GM_p}{r_p} \left(\sum_{n=0}^{\infty} \left(\frac{r}{r_p} \right)^n P_n(\cos\alpha) - \frac{r}{r_p} \cos\alpha - 1 \right) . \qquad (16)$$

Note that the second and third terms within parenthesis are precisely the first two terms of the series (with opposite signs), so we obtain Ω_t expressed as a series of Legendre polynomials:

$$\Omega_t(\alpha) = \frac{GM_p}{r_p} \sum_{n=2}^{\infty} \left(\frac{r}{r_p} \right)^n P_n(\cos\alpha)\,. \tag{17}$$

Given that $r \ll r_p$, we can approximate Ω_t with the first term of the series (as n increases we have increasingly negligible terms, as it will be shown below), obtaining the tide rising potential in polynomial form of harmonic degree $n = 2$:

$$\Omega_t(\alpha) = \frac{GM_p}{r_p} \left(\frac{r}{r_p} \right)^2 P_2(\cos\alpha)\,, \tag{18}$$

where $P_2(\cos\alpha) = \frac{3}{2}\cos^2\alpha - \frac{1}{2}$ is the Legendre polynomial of degree $n = 2$.

To show that this approximation is correct in the case of the moons of Uranus, we can compute the first two terms of Eq. (17) for the nearest moon, Cordelia, for $\alpha = 0\,°$. Using $M_p = M_{Ur} = 8.68 \cdot 10^{25}\,kg$ [Jacobson et al., 1992], $r = R$ from Table 1 and $r_p = a$ from Table 5, we obtain:

- Term with $n = 2$: $\Omega_t(0\,°) = 20.673\,\frac{J}{kg}$;
- Term with $n = 3$: $\Omega_t(0\,°) = 0.009\,\frac{J}{kg}$;

thus confirming that the contributions of terms with degrees $n \geq 3$ are negligible compared to the first one ($n = 2$).

3.3 Tidal Love numbers

With the hypothesis of elasticity, the tide rising potential Ω_t (18) generates a deformation of the moon in O as a displacement of the surface with vertical (radial) component U and horizontal (tangential) component V, whose directions are shown in Figure 4.
A. E. H. Love proposed in [Love, 1909] that, for small deformations, the vertical displacement is proportional by a certain factor h to the tide rising potential according to:

$$U = h\,\frac{\Omega_t}{g}\,, \tag{19}$$

where g is the mean surface gravity of the moon (constant).
Love also hypothesized that the deformation generated by tide rising potential induces a variation in the total potential acting on the considered point that, for small deformations, is proportional by a factor k to Ω_t itself:

$$\Omega' = k\,\Omega_t\,. \tag{20}$$

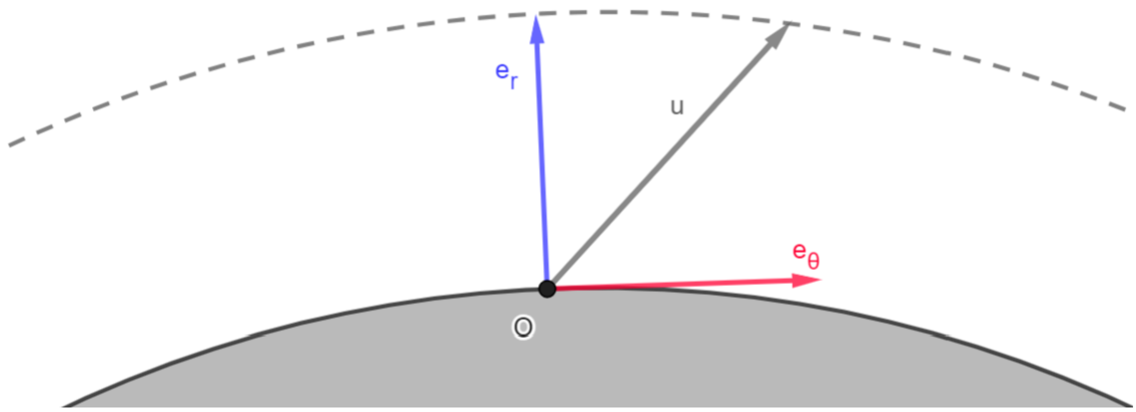

Figure 4: *Graphical representation of a surface displacement $\vec{u}$ induced by Ω_t on a generic point O on the surface of the moon. The continuous line represents the surface before the deformation while the dashed line represents the surface after the deformation; vertical displacement U is directed like the radial unit vector $\widehat{e_r} = \widehat{r}$ while horizontal displacement V is directed like the tangential one $\widehat{e_\theta}$.*

A similar relation to Eq. (19) was considered afterwards by T. Shida in [Shida, 1912] for the horizontal displacement, with a proportionality factor l:

$$V = l\,\frac{\Omega_t}{g}\,. \tag{21}$$

The dimensionless coefficients h, k and l are now known as *tidal Love numbers* or just Love numbers (vertical, potential and horizontal respectively) and they fully describe the deformative response to tidal forces exerted on the moon by other perturbing masses [Munk and MacDonald, 1975, Melchior, 1983]. For a perfectly rigid body, $h = k = l = 0$. Love numbers are also indicated as h_2, k_2 and l_2 to highlight the degree 2 of the polynomial tide rising potential which they refer to (if we consider a general tide rising potential of degree n instead, the notation would be h_n, k_n and l_n).

For an elastic, homogeneous and incompressible planetary body, W. Thomson found in [Thomson, 1863] an analytical relation for all Love numbers as follows:

$$h = \frac{h_f}{1 + \dfrac{19}{2}\dfrac{\mu}{\rho g R}}\,, \tag{22}$$

where μ is the shear modulus (or rigidity) of the moon and h_f (k_f for k, l_f for l) is the fluid Love number, *i. e.* the Love number associated to a planetary body with the same radius, density and surface gravity but completely fluid ($\mu = 0$).

For a spherically symmetric planetary model, h shall be a function in the form:

$$h = h\left(R_i,\, \mu_i,\, \rho_i\right), \tag{23}$$

where R_i are the radii of the internal layers, μ_i are their shear moduli and ρ_i are their densities. However, for a general spherically symmetric model no analytical solution for h is known, except for very simple particular cases [Wu and Ni, 1996].

The dimensionless number:

$$F = \frac{\mu}{\rho\, g\, R}\,, \tag{24}$$

introduced here for the first time, gives the ratio between the amplitude of elastic and gravitational forces acting on the planet. Note that if elasticity is more relevant than gravity, *i. e.* $F \gg 1$, Eq. (22) becomes:

$$\frac{h}{h_f} \simeq \frac{1}{\dfrac{19}{2}F} \simeq 0.1\, F^{-1}\,. \tag{25}$$

For example, for a relatively large body like the Earth, this approximation is not valid because gravity and elasticity have a comparable importance and condition $F \gg 1$ is not met. Indeed, for the Earth, $F \simeq 0.2$ as first noted by Love in [Love, 1911].

As showed in [Wu and Peltier, 1982], in order to obtain Eq. (22) consider the following three equations that fully describe the general problem of an elastic, homogeneous and compressible body:

- *Constitutive law for elastic bodies*:

$$\tau_{ij} = 2\mu\epsilon_{ij} + \lambda\epsilon_{kk}\delta_{ij}\,, \tag{26}$$

  where τ_{ij} is the stress tensor, ϵ_{ij} is the strain tensor, μ is the shear modulus, λ is the Lamé constant and δ_{ij} is the Kronecker delta;

- *Equation of momentum conservation*:

$$-\rho\vec{\nabla}\phi - \vec{\nabla}(\vec{u}\cdot\rho g\widehat{r}) + \frac{\partial\tau_{ij}}{\partial x_i} = 0\,, \tag{27}$$

  where ρ is the density, $\phi = \Omega_t + \Omega'$ is the total perturbative potential and $\vec{u}$ is the displacement vector. The first two terms are the forces per unit volume of gravity and advection while the last term is the force per unit surface of stress;

- *Poisson equation for gravitational potential*:

$$\nabla^2\phi = 4\pi G\rho_1\,, \tag{28}$$

where ρ_1 is the density variation due to tidal deformation.

For an incompressible body: $\rho_1 = 0$, and Eq. (28) becomes:

$$\nabla^2\phi = 0\,. \tag{29}$$

In the case of an incompressible body, we also use Love's hypothesis: $\vec{\nabla}\cdot\vec{u} \to 0$ and $\lambda \to \infty$ so as that their product is finite:

$$\lambda\vec{\nabla}\cdot\vec{u} \to \Pi\,, \tag{30}$$

where Π is the mean normal stress.
Thanks to this fact and in addition to the definition of infinitesimal strain tensor:

$$\epsilon_{ij} = \frac{1}{2}\left(\frac{\partial u_i}{\partial x_j} + \frac{\partial u_j}{\partial x_i}\right)\,, \tag{31}$$

applying the divergence to Eq. (26) we obtain:

$$\frac{\partial\tau_{ij}}{\partial x_i} = \vec{\nabla}\Pi + \mu\vec{\nabla}\times\vec{\nabla}\times\vec{u}\,. \tag{32}$$

Inserting the relation (32) in Eq. (27) we obtain:

$$-\frac{\rho}{\mu}\vec{\nabla}^2\left(\phi + g\vec{u}\cdot\widehat{r} - \frac{\Pi}{\rho}\right) = 0\,, \tag{33}$$

that has solutions that can be expressed as a harmonic decomposition for spherical simmetry in terms of Legendre polynomials $P_n(\cos\theta)$, where θ is the colatitude referred to the position of the tide rising body.
In particular, both $\vec{u}$ and ϕ can be decomposed as:

$$\vec{u}(r,\theta) = \sum_{n=0}^{\infty}\left[U_n(r)P_n(\cos\theta)\widehat{e_r} + V_n(r)\frac{\partial}{\partial\theta}P_n(\cos\theta)\widehat{e_\theta}\right]\,, \tag{34}$$

$$\phi(r,\theta) = \sum_{n=0}^{\infty}\phi_n(r)P_n(\cos\theta)\,, \tag{35}$$

where $U_n(r)$ and $V_n(r)$ are the harmonic coefficients of the vertical and horizontal components of the displacement, $\widehat{e_r} = \widehat{r}$ and $\widehat{e_\theta}$ are the unit radial and tangential vectors and $\phi_n(r)$ is the harmonic component of the perturbative potential.

As shown in [Wu and Peltier, 1982], inserting these solutions into Eq. (29) and Eq. (33) we reach a set of ordinary differential equations for $U_n(r)$, $\phi_n(r)$ and $V_n(r)$ that, solved and compared to their general definitions of degree n:

$$U_n(r) = h_n \frac{\Omega_n^t(r)}{g}\,, \tag{36}$$

$$\Omega_n'(r) = k_n\, \Omega_n^t(r)\,, \tag{37}$$

$$V_n(r) = l_n \frac{\Omega_n^t(r)}{g}\,, \tag{38}$$

where Ω_n^t is the tide rising potential Ω_t of harmonic degree n, allow us to obtain the relation (22) for h_2, k_2 and l_2 in the special case of a homogeneous and incompressible model.

4 Methods

With fixed radius R, Love numbers are function of only μ and ρ, as through inserting the relations (2) and (1) into Eq. (22) we obtain:

$$h = \frac{h_f}{1 + \frac{57}{8} \frac{\mu}{G\pi\rho^2 R^2}} \,. \tag{39}$$

For their evaluation, we used the *Wolfram Mathematica* [Wolfram Research Inc, 2024] software to obtain a 3D plot of (39) in μ and ρ variables, for fixed values of R for each moon in Tables 1, 2 and 3.
Fluid Love numbers values h_f, k_f and l_f for elastic and incompressible spherical planets are taken from [Wu and Peltier, 1982]:

$$h_f = \frac{5}{2}; \quad k_f = \frac{3}{2}; \quad l_f = \frac{5}{4} \,. \tag{40}$$

The values used to plot the range of density ρ, variable for each moon, are taken from uncertainties ranges of Tables 1, 2 and 3.
The plotting range of shear modulus μ is obtained considering as mean values those reported in [Hammond, 2020] and [Hay et al., 2022], approximately around $3.3 - 3.5$ GPa (estimated values for Jupiter's moons Europa and Ganymede, planetary bodies formed by the same mixed materials of ice and rocks of the moons of Uranus).

As an example of Love numbers evaluation for inner, major and outer moons, Figures 5, 6 and 7 show the plots of h, k and l for the moons Cordelia, Umbriel and Francisco, respectively. The *Wolfram Mathematica* codes that we used for the evaluations are reported in Appendix B, followed by some short comments and indications of possible improvements.
As expected from (39), Love numbers values increase with increasing values of density and decrease with increasing values of shear modulus.

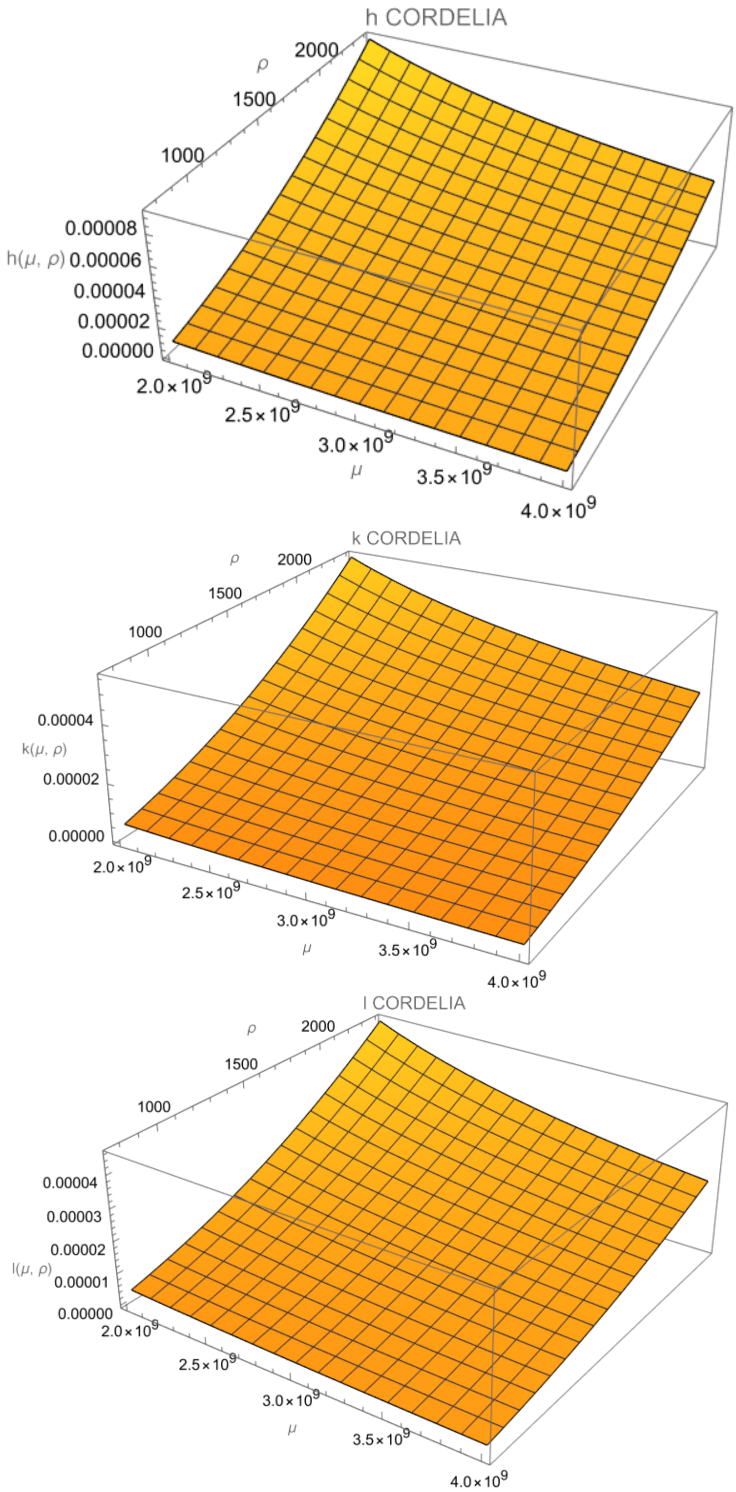

Figure 5: *Plot of Cordelia's Love numbers. Density range ρ is taken from Table 1 and reported in units of $\frac{kg}{m^3}$. Shear modulus range μ is reported in units of Pa.*

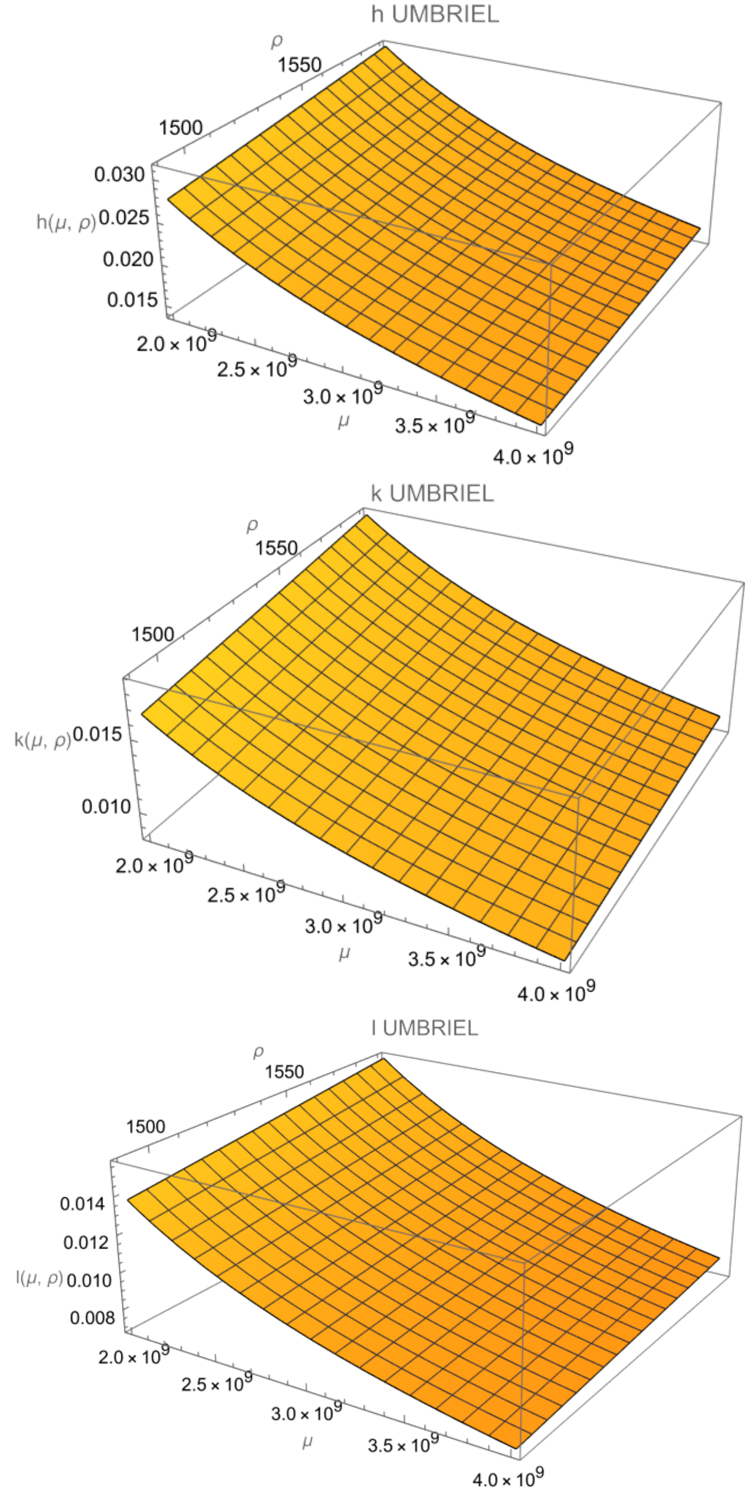

Figure 6: *Plot of Umbriel's Love numbers. Density range ρ is taken from Table 2 and reported in units of $\frac{kg}{m^3}$. Shear modulus range μ is reported in units of Pa.*

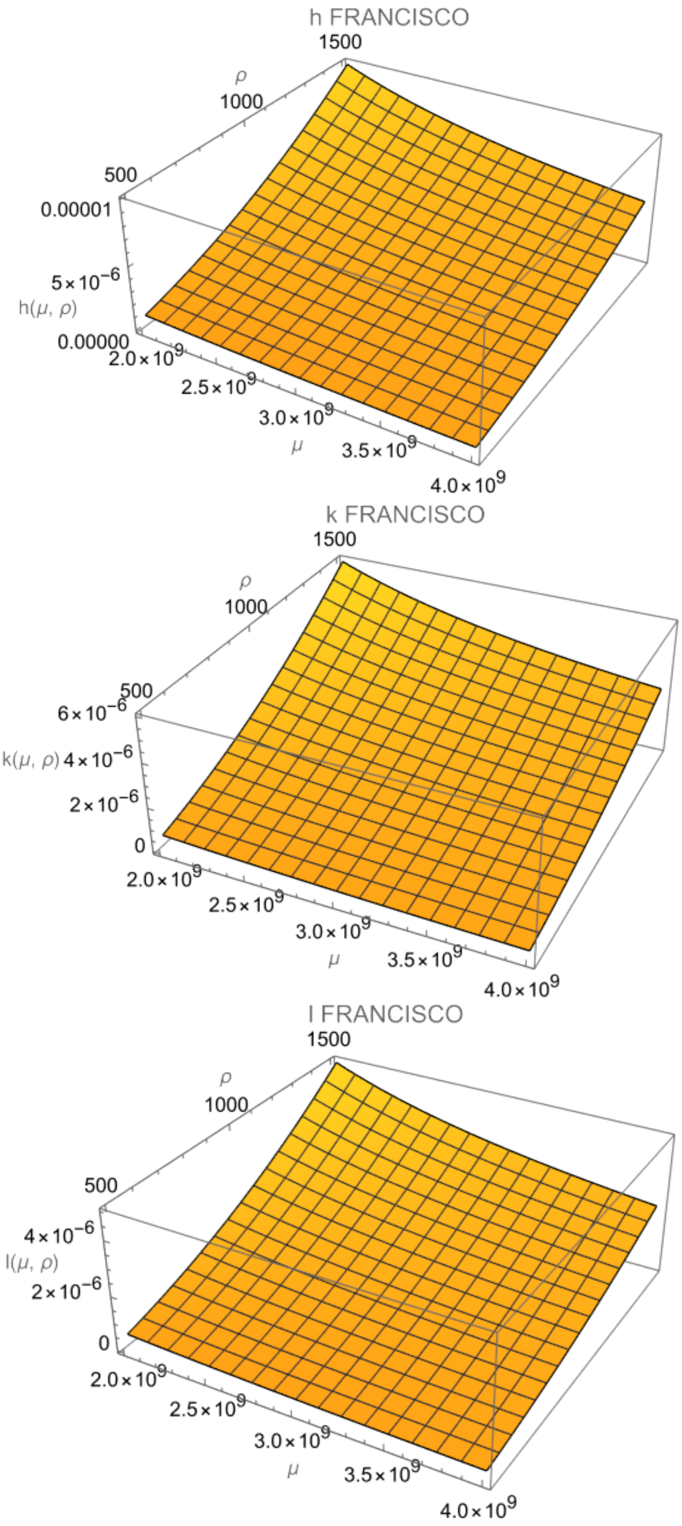

Figure 7: *Plot of Francisco's Love numbers. Density range ρ is taken from Table 3 and reported in units of $\frac{kg}{m^3}$. Shear modulus range μ is reported in units of Pa.*

5 Results

5.1 Love numbers evaluation

It is possible to extrapolate from the previous plots the values of h, k and l using the most appropriate values of density and shear modulus for each moon. Love numbers evaluated for the Uranian satellites are reported in Tables 6, 7 and 8 and k is plotted in Figures 8, 9 and 10 for a graphic comparison; h and l have the same plot as k due to similar (39) relation, up to different constants h_f and l_f, so they are not reported.

Love numbers of major moons are compared in Table 7 to Love numbers of two elastic homogeneous incompressible Earth models, computed by (39) assuming two different values of mean shear modulus:

- $R_{Earth} = 6371\,km$;
- $\rho_{Earth} = 5.515\,\frac{g}{cm^3}$;
- $\bar{\mu}_1 = 146\,GPa$ [Zhang, 1992];
- $\bar{\mu}_2 = 117.66\,GPa$ [Poulsen, 2009];

and to those of an elastic homogeneous incompressible Moon model, assuming:

- $R_{Moon} = 1737\,km$;
- $\rho_{Moon} = 3.344\,\frac{g}{cm^3}$ [Zhang, 1992];
- $\bar{\mu}_{Moon} = 66.8\,GPa$ [Zhang and Shen, 1988];

The largest Love numbers values we obtain are those of the major moons, especially Titania and Oberon, that are also the greatest moons in terms of both radius and mass. While their Love numbers are not comparable with the values that we obtain for the two models of Earth, they are instead comparable to those of the homogeneous model of Moon, a fact that suggests a similarity in their tidal response even though their dimensions and assumed composition are different.
For inner and outer moons, the order of magnitude of their Love numbers is 10^{-6} - 10^{-5}, that clearly indicates a small tidal response. The only satellites of this type that have greater Love numbers are Puck (for inner moons) and Sycorax (for outer moons), with order of magnitude of 10^{-4}.

Moon	***h*** (10^{-3})	***k*** (10^{-3})	***l*** (10^{-3})
Cordelia	0.02351	0.01410	0.01175
Ophelia	0.00561	0.00336	0.00280
Bianca	0.00935	0.00561	0.00467
Cressida	0.01489	0.00893	0.00744
Desdemona	0.01261	0.00757	0.00631
Juliet	0.02335	0.01401	0.01167
Portia	0.06952	0.04171	0.03476
Rosalind	0.02270	0.01362	0.01135
Cupid	0.00175	0.00105	0.00088
Belinda	0.01850	0.01110	0.00925
Perdita	0.00487	0.00292	0.00243
Puck	0.10493	0.06296	0.05247
Mab	0.00311	0.00187	0.00156

Table 6: **Love numbers of inner moons**
Love numbers of inner moons were obtained using the density of each moon from Table 1 and the average shear modulus $\bar{\mu} = 3.4\,GPa$.

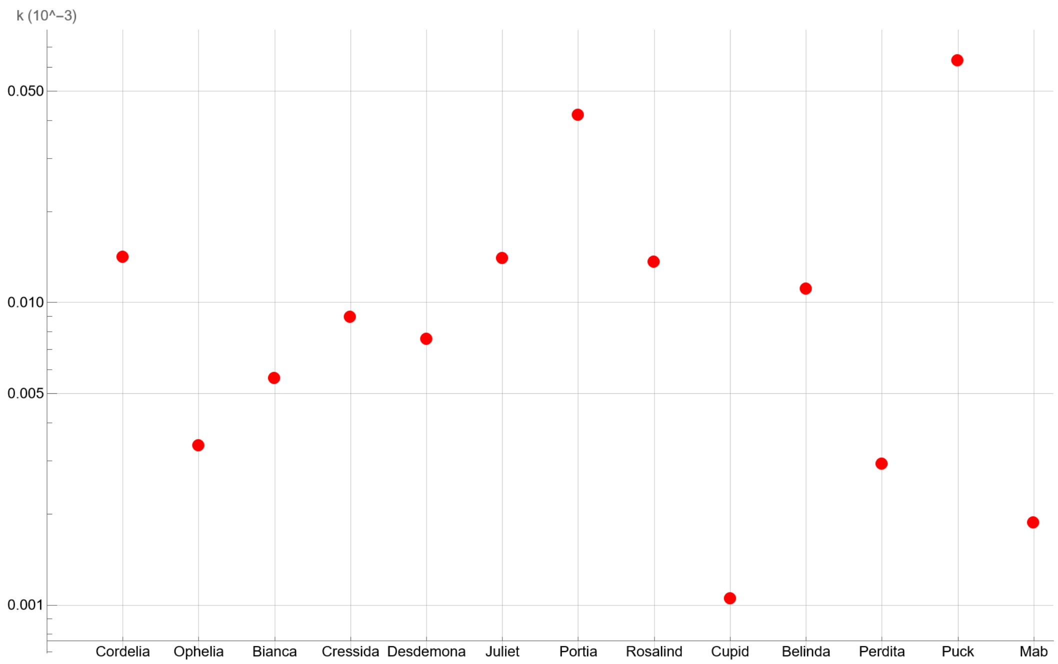

Figure 8: *Graphical comparison of potential Love number k for inner moons, plotted in logarithmic scale.*

Moon	h	k	l
Miranda	0.00159	0.00095	0.00079
Ariel	0.01663	0.00998	0.00832
Umbriel	0.01741	0.01045	0.00871
Titania	0.03742	0.02245	0.01871
Oberon	0.03489	0.02093	0.01744
Earth $[\bar{\mu}_1]$	0.58953	0.35372	0.29477
Earth $[\bar{\mu}_2]$	0.49789	0.29873	0.24894
Moon	0.03659	0.02196	0.01830

Table 7: **Love numbers of major moons**
Love numbers of major moons were obtained using the density of each moon from Table 2 and the average shear modulus $\bar{\mu} = 3.4\,GPa$. *They are compared to Love numbers obtained for incompressible homogeneous Earth and Moon models.*

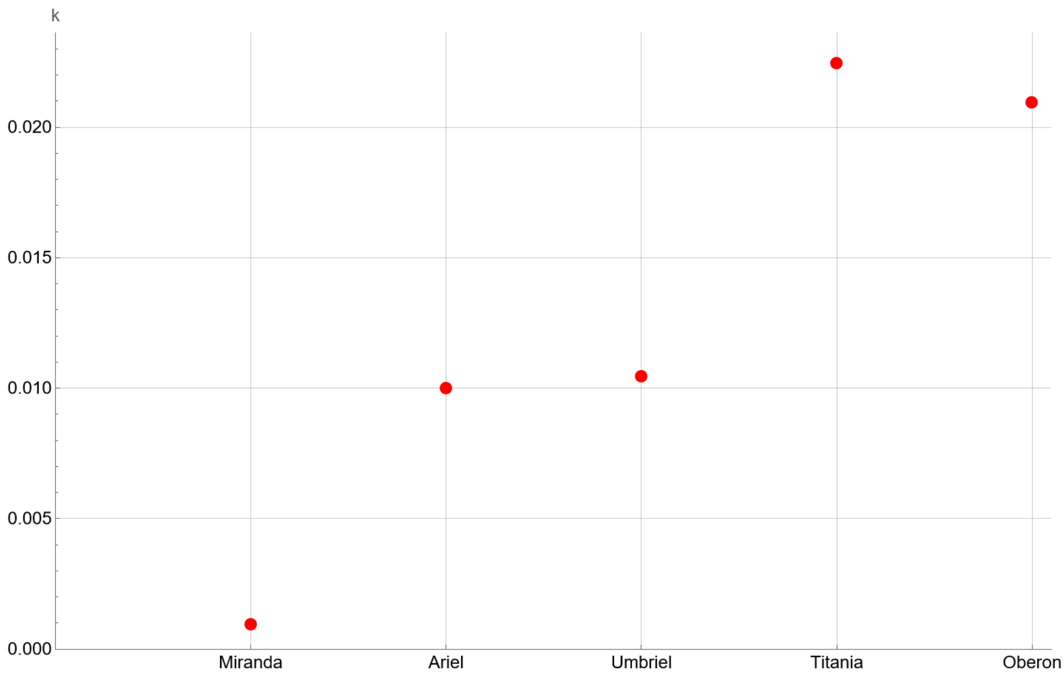

Figure 9: *Graphical comparison of potential Love number k for major moons.*

Moon	$\boldsymbol{h}$ (10^{-3})	$\boldsymbol{k}$ (10^{-3})	$\boldsymbol{l}$ (10^{-3})
Francisco	0.00262	0.00157	0.00131
Caliban	0.02803	0.01682	0.01401
Stephano	0.00554	0.00332	0.00277
Trinculo	0.00175	0.00105	0.00088
Sycorax	0.12163	0.07298	0.06082
Margaret	0.00216	0.00130	0.00108
Prospero	0.01352	0.00811	0.00676
Setebos	0.01246	0.00747	0.00623
Ferdinand	0.00216	0.00130	0.00108

Table 8: **Love numbers of outer moons**
Love numbers of outer moons were obtained using the density of each moon from Table 3 and the average shear modulus $\bar{\mu} = 3.4\,GPa$.

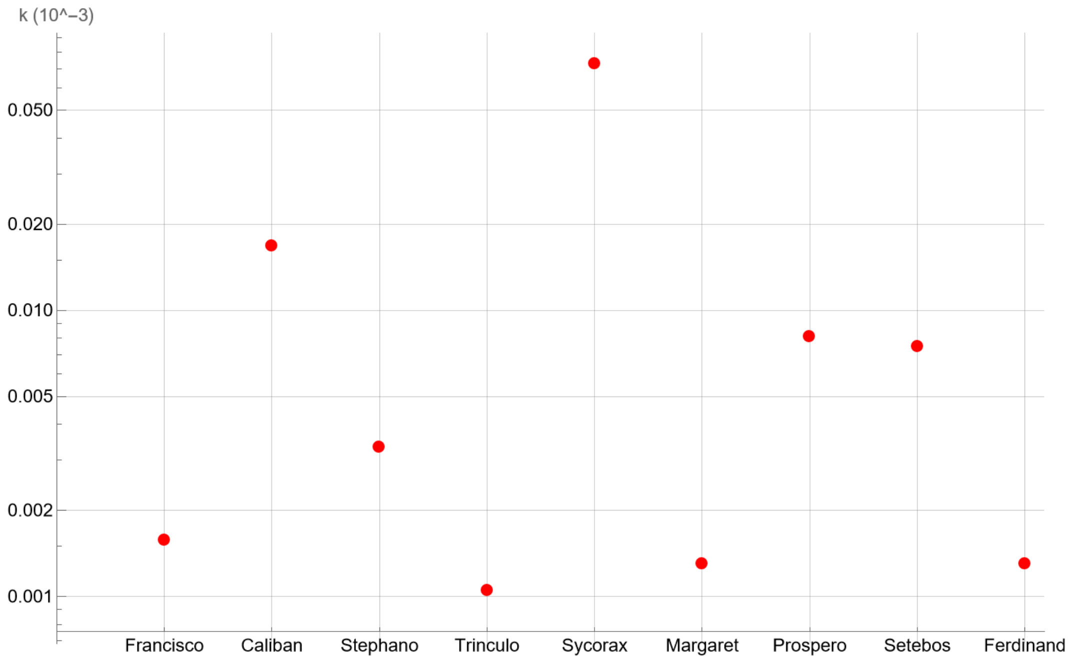

Figure 10: *Graphical comparison of potential Love number* k *for outer moons, plotted in logarithmic scale.*

5.2 Vertical displacements evaluation

It is also possible to evaluate the amplitude of vertical deformations U caused by the mass of Uranus M_{Ur} at the surface of each moon as follows.
Inserting (18) into Eq. (19) we obtain:

$$U = \frac{h}{g}\frac{GM_p}{2r_p}\left(\frac{r}{r_p}\right)^2\left(3\cos^2\alpha - 1\right) , \tag{41}$$

where:

- $M_p = M_{Ur} = 8.68 \cdot 10^{25}\, kg$ [Jacobson et al., 1992];
- $r = R$ radius of the moon;
- $r_p = a$ semi-major orbital axis.

Using h values for each moon from Tables 6, 7 and 8, we can evaluate the *equatorial vertical displacement* U_{eq} for $\alpha = 0\,^\circ$ as:

$$U_{eq} = \frac{h}{g}\frac{GM_{Ur}}{a}\left(\frac{R}{a}\right)^2 , \tag{42}$$

and the *polar vertical displacement* U_{pol} for $\alpha = 90\,^\circ$ as:

$$U_{pol} = -\frac{h}{g}\frac{GM_{Ur}}{2a}\left(\frac{R}{a}\right)^2 = -\frac{U_{eq}}{2} , \tag{43}$$

where the $-$ sign means that at the poles the equilibrium surface is displaced downwards.

The evaluated values of U_{eq} and U_{pol} are reported in Tables 9, 10 and 11.
For inner moons, due to the dependency of displacements from a^{-3} and g^{-1} of Eq. (42) and Eq. (43), we obtain values of U_{eq} in a range from $0.08\,cm$ up to almost $43\,cm$; in fact, for the largest ones we have displacements of a few tens of centimeters, like Portia and Cupid, that show a remarkable tidal response.
For major moons, even if their Love number h are the largest, we have smaller values of displacements than those of the inner satellites, due to both greater distance from Uranus and surface gravity; among these moons, Ariel has the greatest equatorial displacement, of about $1.89\,cm$.
A different case is the one of outer moons: they are so far from the planet that the tidal vertical deformation of their surface, computed with the previous approximations, are of the order of magnitude of 10^{-11} - $10^{-7}\,m$, practically negligible.

Moon	$\boldsymbol{U_{eq}}$ (cm)	$\boldsymbol{U_{pol}}$ (cm)
Cordelia	5.28	−2.64
Ophelia	2.45	−1.23
Bianca	3.26	−1.63
Cressida	8.41	−4.21
Desdemona	5.38	−2.69
Juliet	15.47	−7.74
Portia	42.98	−21.49
Rosalind	5.51	−2.76
Cupid	0.08	−0.04
Belinda	6.24	−3.12
Perdita	0.34	−0.17
Puck	32.27	−16.13
Mab	0.08	−0.04

Table 9: **Vertical displacements of inner moons**
Equatorial and polar vertical displacements of inner moons are obtained using Eq. (42) and Eq. (43), with radius values R taken from Table 1 and semi-major orbital axis a taken from Table 5.

Moon	$\boldsymbol{U_{eq}}$ (cm)	$\boldsymbol{U_{pol}}$ (cm)
Miranda	0.31	−0.15
Ariel	1.89	−0.94
Umbriel	0.73	−0.36
Titania	0.44	−0.22
Oberon	0.16	−0.08

Table 10: **Vertical displacements of major moons**
Equatorial and polar vertical displacements of major moons are obtained using Eq. (42) and Eq. (43), with radius values R taken from Table 2 and semi-major orbital axis a taken from Table 5.

Moon	$\boldsymbol{U_{eq}}$ ($10^{-10}\,m$)	$\boldsymbol{U_{pol}}$ ($10^{-10}\,m$)
Francisco	76.48	-38.24
Caliban	0.57	-0.28
Stephano	36.54	-18.27
Trinculo	5.32	-2.66
Sycorax	1042.97	-521.49
Margaret	1.49	-0.75
Prospero	16.42	-8.21
Setebos	11.52	-5.76
Ferdinand	0.53	-0.26

Table 11: **Vertical displacements of outer moons**
Equatorial and polar vertical displacements of outer moons are obtained using Eq. (42) and Eq. (43), with radius values R taken from Table 3 and semi-major orbital axis a taken from Table 5.

6 Discussion

It is important to recall that the results obtained in the previous Section are based on simplified approximations that however reflect, at least on a first level of study, the physical properties of the moons of Uranus and allow us to obtain a first, very rough, description of their tidal response. Nevertheless, reality is more complex and the approximations used in this dissertation can be improved due to the following observations.

On shape and structure

The approximation of spherical shape we used is not the better choice for all the moons of Uranus. In fact, the best shape model of some of the inner satellites is not spherical but ellipsoidal (as prolate spheroid): some evident examples of this are Ophelia, Cupid and Mab, as shown in Figure 11, and an evaluation of their three dimensions as a prolate spheroid has been made by E. Karkoschka in [Karkoschka, 2001]. Despite that, the hypothesis of homogeneous internal structure is quite reasonable as from their dimensions and from available physical data they do not seem to have an internal differentiation.

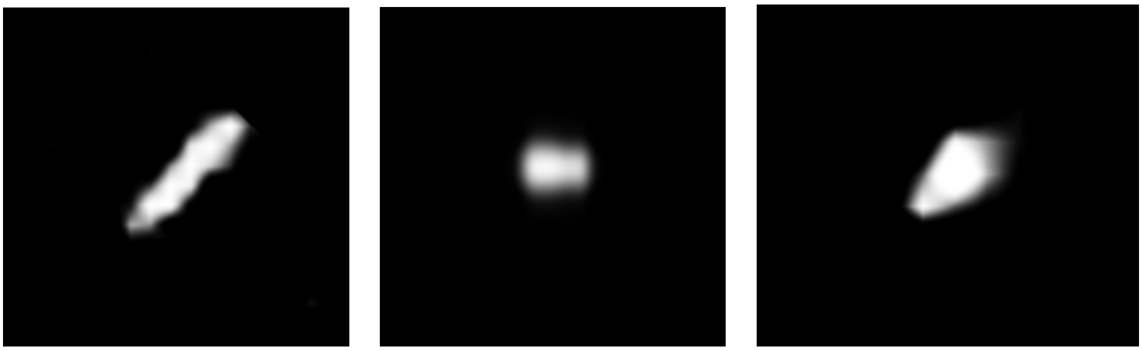

Figure 11: *From left to right, Ophelia captured by the Voyager 2 Spacecraft and Cupid and Mab captured by the Hubble Space Telescope. Jan. 21, 1986; 2003. NASA.*

On the other hand, if we consider major moons it is realistic to assume the spherical shape approximation, as visible in Figure 12, but not the hypothesis of homogeneity. In fact, due to their physical data, internal differentiation processes are plausible and many papers already hypothesize this scenario: in [Castillo-Rogez et al., 2023] the authors present a two-layered model for Miranda (rocky core; ice shell) and three-layered models for Ariel, Umbriel, Titania and Oberon (rocky core; thick ocean; ice shell); for Titania and Oberon, the presence of a subsurface ocean was already been presented in [Hussmann et al., 2006]. These models should be considered since the chemical species confirmed to be on these moons, like ammonia [Grundy et al., 2006], have the property of lowering the melting point of water, allowing the presence of liquid water oceans. In addition to it, some of the major moons, like Ariel, present formations on the surface that can be related to past cryovolcanism activity, a phenomenon that goes hand-in-hand with the possible presence of subsurface oceans [Carroll, 2019].

Figure 12: *From left to right, Ariel, Titania and Oberon captured by the Voyager 2 Spacecraft. Jan. 24, 1986. NASA/JPL.*

In particular, J. Castillo-Rogez et al. have also evaluated the potential Love number k for the differentiated models that they proposed, reported in Table 12. Comparing these values to the ones we reported in Table 7, recalled in Table 12, it follows that k for homogeneous models underestimates k for differentiated models so detecting its value for each moon in the future is important to understand the level of internal differentiation of these bodies.

Moon	***k* (Castillo-Rogez)**	***k* (Table 7)**
Miranda	0.0019	0.00095
Ariel	$0.016 - 0.164$	0.00998
Titania	0.24	0.02245

Table 12: **Potential Love numbers k for differentiated models of major moons** *Potential Love number k evaluated in [Castillo-Rogez et al., 2023] for three of the major moons of Uranus, compared with the values we obtained in Table 7. Castillo-Rogez considered Miranda with a two-layered model (without ocean) and Ariel and Titania with a three-layered model (with a subsurface ocean).*

While if we know the interior of a planetary body then we know its Love numbers, the knowledge of Love numbers does not allow us to infer exactly its internal structure, not even for a homogeneous sphere. Nevertheless, as showed in [Zhang, 1992], Love number k increases with increasing radius of the core: this means that, comparing future-detected values with computed ones for many models, it will be possible to identify the class of models that provide the best fit with measured Love numbers, providing some indication about the size of the core.

On compressibility

Another hypothesis that can be improved is the one of incompressibility: although our knowledge about these moons is poor, it is not very realistic to consider them as incompressible because for solid planetary bodies compressibility can be significant.

The most relevant studies that developed this perspective have been carried out by T.A. Hurford [Hurford and Greenberg, 2002, Hurford, 2005, Hurford et al., 2006]. In [Hurford and Greenberg, 2002], they considered for Eq. (27) an additional term depending on the Lamé constant λ, that has a finite real value for compressible bodies (for example, for rocky bodies $\lambda \sim \mu$). Repeating the process shown in Section 3.3 with functions written as Legendre polynomials series, it is possible to reach a relation for the vertical Love number h through the comparison of the total perturbative potential ϕ with its definition; note that now ϕ has more terms than in the incompressible case.
We have chosen not to report here neither the full discussion on the topic nor the relation for h due to their complexity, but please refer to [Hurford and Greenberg, 2002, Hurford et al., 2006].

7 Conclusions

Having previously discussed the physical properties of the satellites, presented the approximated model we adopted and showed the analysis we carried out, I can now recall the results obtained in this thesis:

- at first, through the 3D plots in Section 4 we have observed the combined dependence of Love numbers on density and on shear modulus of the bodies they refer to. These parameters can be modified in order to adapt the model to the most suitable values for each moon;

- then, we have evaluated the Love numbers for all the moons, obtaining values of the order of 10^{-6} - 10^{-5} for the small ones and values of the order of 10^{-3} - 10^{-2} for the major ones. For the former, we have inferred that they have a limited tidal response despite their composition is mainly based on icy materials. For the latter, we have shown a similarity in tidal response with a homogeneous model of our Moon and highlighted that k values for homogeneous models underestimate k values for differentiated models;

- in the end, we have also computed the values of vertical displacements at the surface of the moons, caused by the tidal influence of Uranus. For the inner moons, very close to the planet, we have obtained values in a range from a few centimeters up to a few tens of centimeters. For the major ones, the maximum value of surface displacement is $1.89\,cm$, for Ariel. The outer moons have negligible displacements due to their greater distance from Uranus.

The future detection of Love numbers of these planetary bodies will give us new tools to investigate their internal differentiation and to understand if the hypothesis of subsurface oceans for the major satellites are realistic: only through space missions like *NASA Uranus Orbiter and Probe* we will be able to discover the possible structure of the moons of Uranus.

Acknowledgments

I wish to thank Daniele Melini (*INGV*, Rome) and Anastasia Consorzi (*DIFA, Alma Mater Studiorum - Università di Bologna*) for discussion and encouragement.
This work was partly funded by the Italian Space Agency (ASI) through agreement no. 2024-5-HH.0.

Appendix

A. Errors evaluation

Radius R and mass M values, reported in Tables 1 and 2 in Section 2.2, were evaluated in cited papers through the analysis of the original images captured by *NASA Voyager 2* and through later processing. Due to this fact, we can not rule out the possibility that their computed uncertainties are not independent: therefore, we have chosen to evaluate uncertainties on ρ and g values through the propagation of uncertainty as upper limits and not in quadrature [Taylor, 1997].

As discussed in [Taylor, 1997], if f is a function depending on variables a, b, ..., z so that $f = f\,(a,\, b,\, ...,\, z)$, the upper limit of uncertainty on the value of f can be evaluated as:

$$\Delta f = \left|\frac{\partial f}{\partial a}\right| \Delta a + \left|\frac{\partial f}{\partial b}\right| \Delta b + ... + \left|\frac{\partial f}{\partial z}\right| \Delta z\,,$$

where Δa, Δb, ..., Δz are the uncertainties on a, b, ..., z values.

Considering Eq. (1) where ρ is a function of radius R and mass M: $\rho = \rho\,(R,\, M)$, we have obtained the uncertainty on ρ as:

$$\Delta \rho = \left|\frac{\partial \rho}{\partial R}\right| \Delta R + \left|\frac{\partial \rho}{\partial M}\right| \Delta M\,,$$

where ΔR is the uncertainty on R and ΔM is the uncertainty on M.
Explicitly:

$$\Delta \rho = \frac{1}{\frac{4}{3}\pi R^3}\left(3M\frac{\Delta R}{R} + \Delta M\right)\,.$$

Considering Eq. (2) where g is a function of radius R and mass M: $g = g\,(R,\, M)$, we have obtained the uncertainty on g as:

$$\Delta g = \left|\frac{\partial g}{\partial R}\right| \Delta R + \left|\frac{\partial g}{\partial M}\right| \Delta M\,.$$

where ΔR is the uncertainty on R and ΔM is the uncertainty on M.
Explicitly:

$$\Delta g = \frac{G}{R^2}\left(2M\frac{\Delta R}{R} + \Delta M\right)\,.$$

B. Wolfram Mathematica Codes

In order to improve the evaluation of tidal Love numbers we carried out, in this Appendix we report all the *Wolfram Mathematica* [Wolfram Research Inc, 2024] codes we used to obtain the plots showed in Section 4.
For example, it is possible to try different ranges of shear modulus μ, based on different composition models, or different ranges of density ρ.

```
(*CORDELIA*)
(* Radius R [m] , Density rho [kg/m^3], Shear modulus mu [kg/m s^2], G [m^3/kg s^2]*)
R = 21*10^3;
G = 6.67*10^(-11);

kf = 3/2;
hf = 5/2;
lf = 5/4;

k[mu_, rho_] := kf/(1 + (57/8)*(mu/(G*π*(rho^2)*(R^2))));
h[mu_, rho_] := hf/(1 + (57/8)*(mu/(G*π*(rho^2)*(R^2))));
l[mu_, rho_] := lf/(1 + (57/8)*(mu/(G*π*(rho^2)*(R^2))));

Plot3D[k[mu, rho], {mu, 2*10^9, 4*10^9}, {rho, 0.75*10^3, 2.39*10^3},
 AxesLabel → {"μ", "ρ", "k(μ, ρ)"}, PlotLabel → "k CORDELIA"]
Plot3D[h[mu, rho], {mu, 2*10^9, 4*10^9}, {rho, 0.75*10^3, 2.39*10^3},
 AxesLabel → {"μ", "ρ", "h(μ, ρ)"}, PlotLabel → "h CORDELIA"]
Plot3D[l[mu, rho], {mu, 2*10^9, 4*10^9}, {rho, 0.75*10^3, 2.39*10^3},
 AxesLabel → {"μ", "ρ", "l(μ, ρ)"}, PlotLabel → "l CORDELIA"]
```

Figure 13: *Code used to obtain the 3D plot of h, k and l for Cordelia, with its value of R and its ranges of μ and ρ already inserted.*

```
(*UMBRIEL*)
(* Radius R [m] , Density rho [kg/m^3], Shear modulus mu [kg/m s^2], G [m^3/kg s^2]*)
R = 584.7*10^3;
G = 6.67*10^(-11);

kf = 3/2;
hf = 5/2;
lf = 5/4;

k[mu_, rho_] := kf/(1+(57/8)*(mu/(G*π*(rho^2)*(R^2))));
h[mu_, rho_] := hf/(1+(57/8)*(mu/(G*π*(rho^2)*(R^2))));
l[mu_, rho_] := lf/(1+(57/8)*(mu/(G*π*(rho^2)*(R^2))));

Plot3D[k[mu, rho], {mu, 2*10^9, 4*10^9}, {rho, 1.49*10^3, 1.59*10^3},
 AxesLabel → {"μ", "ρ", "k(μ, ρ)"}, PlotLabel → "k UMBRIEL"]
Plot3D[h[mu, rho], {mu, 2*10^9, 4*10^9}, {rho, 1.49*10^3, 1.59*10^3},
 AxesLabel → {"μ", "ρ", "h(μ, ρ)"}, PlotLabel → "h UMBRIEL"]
Plot3D[l[mu, rho], {mu, 2*10^9, 4*10^9}, {rho, 1.49*10^3, 1.59*10^3},
 AxesLabel → {"μ", "ρ", "l(μ, ρ)"}, PlotLabel → "l UMBRIEL"]
```

Figure 14: *Code used to obtain the 3D plot of h, k and l for Umbriel, with its value of R and its ranges of μ and ρ already inserted.*

```
(*FRANCISCO*)
(* Radius R [m] , Density rho [kg/m^3], Shear modulus mu [kg/m s^2], G [m^3/kg s^2]*)
R = 11*10^3;
G = 6.67*10^(-11);

kf = 3/2;
hf = 5/2;
lf = 5/4;

k[mu_, rho_] := kf/(1+(57/8)*(mu/(G*π*(rho^2)*(R^2))));
h[mu_, rho_] := hf/(1+(57/8)*(mu/(G*π*(rho^2)*(R^2))));
l[mu_, rho_] := lf/(1+(57/8)*(mu/(G*π*(rho^2)*(R^2))));

Plot3D[k[mu, rho], {mu, 2*10^9, 4*10^9}, {rho, 0.5*10^3, 1.5*10^3},
 AxesLabel → {"μ", "ρ", "k(μ, ρ)"}, PlotLabel → "k FRANCISCO"]
Plot3D[h[mu, rho], {mu, 2*10^9, 4*10^9}, {rho, 0.5*10^3, 1.5*10^3},
 AxesLabel → {"μ", "ρ", "h(μ, ρ)"}, PlotLabel → "h FRANCISCO"]
Plot3D[l[mu, rho], {mu, 2*10^9, 4*10^9}, {rho, 0.5*10^3, 1.5*10^3},
 AxesLabel → {"μ", "ρ", "l(μ, ρ)"}, PlotLabel → "l FRANCISCO"]
```

Figure 15: *Code used to obtain the 3D plot of h, k and l for Francisco, with its value of R and its ranges of μ and ρ already inserted.*

Bibliography

[Agnew, 2005] Agnew, D. C. (2005). Earth tides: an introduction. *University of California, San Diego.*

[CarnegieScience, 2024] CarnegieScience (2024). New moons of Uranus and Neptune announced. https://carnegiescience.edu/new-moons-uranus-and-neptune-announced. Accessed: May 15, 2024.

[Carroll, 2019] Carroll, M. (2019). *Ice Worlds of the Solar System: Their Tortured Landscapes and Biological Potential.* Springer International Publishing.

[Cartwright et al., 2015] Cartwright, R. J., Emery, J. P., Rivkin, A. S., Trilling, D. E., and Pinilla-Alonso, N. (2015). Distribution of CO2 ice on the large moons of Uranus and evidence for compositional stratification of their near-surfaces. *Icarus*, 257:428–456.

[Castillo-Rogez et al., 2023] Castillo-Rogez, J., Weiss, B., Beddingfield, C., Biersteker, J., Cartwright, R., Goode, A., Melwani Daswani, M., and Neveu, M. (2023). Compositions and interior structures of the large moons of Uranus and implications for future spacecraft observations. *Journal of Geophysical Research: Planets*, 128(1):e2022JE007432.

[Croft, 1989] Croft, S. (1989). New geologic maps of the uranian satellites Titania, Oberon, Umbriel and Miranda. In *Abstracts of the Lunar and Planetary Science Conference, volume 20, page 205,(1989)*, volume 20.

[Dumas et al., 2003] Dumas, C., Smith, B. A., and Terrile, R. J. (2003). Hubble space telescope NICMOS multiband photometry of Proteus and Puck. *The Astronomical Journal*, 126(2):1080.

[Duncan and Lissauer, 1997] Duncan, M. J. and Lissauer, J. J. (1997). Orbital stability of the Uranian satellite system. *Icarus*, 125(1):1–12.

[French et al., 2024] French, R. G., Hedman, M. M., Nicholson, P. D., Longaretti, P.-Y., and McGhee-French, C. A. (2024). The Uranus system from occultation observations

(1977–2006): Rings, pole direction, gravity field, and masses of Cressida, Cordelia, and Ophelia. *Icarus*, 411:115957.

[Grundy et al., 2006] Grundy, W., Young, L., Spencer, J., Johnson, R., Young, E., and Buie, M. (2006). Distributions of H2O and CO2 ices on Ariel, Umbriel, Titania, and Oberon from IRTF/SpeX observations. *Icarus*, 184(2):543–555.

[Grundy et al., 2003] Grundy, W., Young, L., and Young, E. (2003). Discovery of CO2 ice and leading–trailing spectral asymmetry on the uranian satellite Ariel. *Icarus*, 162(1):222–229.

[Hammond, 2020] Hammond, N. (2020). Estimating the Magnitude of Cyclic Slip on Strike-Slip faults on Europa. *Journal of Geophysical Research: Planets*, 125(7):no–no.

[Hay et al., 2022] Hay, H., Matsuyama, I., and Pappalardo, R. (2022). The high-frequency tidal response of ocean worlds: Application to Europa and Ganymede. *Journal of Geophysical Research: Planets*, 127(5):e2021JE007064.

[Hurford et al., 2006] Hurford, T., Frey, S., and Greenberg, R. (2006). Numerical evaluation of Love's solution for Tidal amplitude. In *Chaotic Worlds: From Order to Disorder in Gravitational N-Body Dynamical Systems*, pages 307–323. Springer.

[Hurford and Greenberg, 2002] Hurford, T. and Greenberg, R. (2002). Tides on a Compressible Sphere: Sensitivity of the h2 Love Number. In *Lunar and Planetary Science Conference*, page 1589.

[Hurford, 2005] Hurford, T. A. (2005). Tides and Tidal Stress: Applications to Europa. *University of Arizona, Tucson.*

[Hussmann et al., 2006] Hussmann, H., Sohl, F., and Spohn, T. (2006). Subsurface oceans and deep interiors of medium-sized outer planet satellites and large trans-neptunian objects. *Icarus*, 185(1):258–273.

[Jacobson, 2023] Jacobson, R. (2023). Update of the Orbits of the Regular Uranian Satellites and the Gravitational Field of the Uranian System. In *AAS/Division for Planetary Sciences Meeting Abstracts*, volume 55, pages 221–02.

[Jacobson et al., 1992] Jacobson, R., Campbell, J., Taylor, A., and Synnott, S. (1992). The masses of Uranus and its major satellites from Voyager tracking data and Earth-based Uranian satellite data. *Astronomical Journal (ISSN 0004-6256), vol. 103, no. 6, June 1992, p. 2068-2078.*, 103:2068–2078.

[Karkoschka, 2001] Karkoschka, E. (2001). Voyager's eleventh discovery of a satellite of Uranus and photometry and the first size measurements of nine satellites. *Icarus*, 151(1):69–77.

[Love, 1909] Love, A. E. H. (1909). The yielding of the Earth to disturbing forces. *Proceedings of the Royal Society of London. Series A, Containing Papers of a Mathematical and Physical Character*, 82(551):73–88.

[Love, 1911] Love, A. E. H. (1911). *Some problems of geodynamics: being an essay to which the Adams prize in the University of Cambridge was adjudged in 1911.* CUP Archive.

[Melchior, 1983] Melchior, P. (1983). *The Tides of the Planet Earth.* Elsevier Science & Technology.

[Mousis, 2004] Mousis, O. (2004). Modeling the thermodynamical conditions in the Uranian subnebula–Implications for regular satellite composition. *Astronomy & Astrophysics*, 413(1):373–380.

[Munk and MacDonald, 1975] Munk, W. and MacDonald, G. (1975). *The Rotation of the Earth: A Geophysical Discussion.* Cambridge Monographs on Mechanics. Cambridge University Press.

[NASA, 2024] NASA (2024). Planetary Satellite Mean Elements. NASA Jet Propulsion Laboratory - *California Institute of Technology.* https://ssd.jpl.nasa.gov/sats/elem/. Accessed: May 1, 2024.

[Plescia, 1987] Plescia, J. (1987). Geological terrains and crater frequencies on Ariel. *Nature*, 327(6119):201–204.

[Poulsen, 2009] Poulsen, S. K. (2009). Tidal Deformation of the Solid Earth - A Finite Difference Discretization. *Niels Bohr Institute, University of Copenhagen.*

[Schenk, 1991] Schenk, P. M. (1991). Fluid volcanism on Miranda and Ariel: Flow morphology and composition. *Journal of Geophysical Research: Solid Earth*, 96(B2):1887–1906.

[Sheppard et al., 2005] Sheppard, S. S., Jewitt, D., and Kleyna, J. (2005). An ultradeep survey for irregular satellites of Uranus: Limits to completeness. *The Astronomical Journal*, 129(1):518.

[Shida, 1912] Shida, T. (1912). On the body tides of the Earth, a proposal for the International Geodetic Association. *Proceedings of the Tokyo Mathematico-Physical Society. 2nd Series*, 6(16):242–258.

[Showalter and Lissauer, 2006] Showalter, M. R. and Lissauer, J. J. (2006). The second ring-moon system of Uranus: discovery and dynamics. *Science*, 311(5763):973–977.

[Smith et al., 1986] Smith, B. A., Soderblom, L., Beebe, R., Bliss, D., Boyce, J., Brahic, A., Briggs, G., Brown, R., Collins, S., Cook, A., et al. (1986). Voyager 2 in the Uranian system: Imaging science results. *Science*, 233(4759):43–64.

[Spada, 2023] Spada, G. (A.A. 2022/2023). Teaching material of "Geodesy" class. *Alma Mater Studiorum - Università di Bologna.*

[Taylor, 1997] Taylor, J. (1997). *Introduction To Error Analysis: The Study of Uncertainties in Physical Measurements.* University Science Books.

[Thomas, 1988] Thomas, P. (1988). Radii, shapes, and topography of the satellites of Uranus from limb coordinates. *Icarus*, 73(3):427–441.

[Thomson, 1863] Thomson, W. (1863). XXVII. On the rigidity of the Earth. *Philosophical Transactions of the Royal Society of London*, (153):573–582.

[Wolfram Research Inc, 2024] Wolfram Research Inc (2024). Mathematica, Version 14.0. Champaign, IL, 2024.

[Wu and Ni, 1996] Wu, P. and Ni, Z. (1996). Some analytical solutions for the viscoelastic gravitational relaxation of a two-layer non-self-gravitating incompressible spherical earth. *Geophysical Journal International*, 126(2):413–436.

[Wu and Peltier, 1982] Wu, P. and Peltier, W. (1982). Viscous gravitational relaxation. *Geophysical Journal International*, 70(2):435–485.

[Zhang, 1992] Zhang, C. (1992). Love numbers of the Moon and of the terrestrial planets. *Earth, Moon, and Planets*, 56(3):193–207.

[Zhang and Shen, 1988] Zhang, C. and Shen, M. (1988). The lunar mean moment of inertia and the size of the Moon's core. *Earth, Moon, and Planets*, 42(2):179–184.